

Self-organized criticality in the Kardar-Parisi-Zhang-equation

Gábor Szabó^{1,2}, Mikko Alava¹, János Kertész²

¹*Helsinki University of Technology, Laboratory of Physics, 02105 HUT, Finland*

²*Budapest University of Technology, Department of Theoretical Physics, H-1111 Hungary*
(November 1, 2018)

Kardar-Parisi-Zhang interface depinning with quenched noise is studied in an ensemble that leads to self-organized criticality in the quenched Edwards-Wilkinson (QEW) universality class and related sandpile models. An interface is pinned at the boundaries, and a slowly increasing external drive is added to compensate for the pinning. The ensuing interface behavior describes the integrated toppling activity history of a QKPZ cellular automaton. The avalanche picture consists of several phases depending on the relative importance of the terms in the interface equation. The SOC state is more complicated than in the QEW case and it is not related to the properties of the bulk depinning transition.

PACS: 05.70.Ln, 64.60-i, 45.70.Ht

One of the more interesting developments in non-equilibrium statistical physics has been the realization that inhomogeneous systems give rise to new, rich behavior compared to those in which translational invariance is present. A prime example thereof is the criticality found in so-called sandpile models, coined 'self-organized' due to the absence of an obvious control parameter [1].

Usual 'self-organized critical' SOC sandpiles have two central features. First, the system is driven very slowly so that individual avalanches occur on a separate, fast time-scale. Second, the drive (like the addition of grains) and the dissipation (loss of grains) occur non-uniformly. Typically the system is forced, on the average, in an uniform fashion but open boundaries create dissipation, in sandpiles via the loss of grains. These two characteristics are the keys to describe, and the earmarks of SOC (for early work see [2]) [3,4].

Essential to a wide class of SOC models is that the movement of grains has a Laplacian character. Consider now the *history* of activity, topplings in such models. The activation of a site means that it has received enough grains, $z(x, t)$, from outside or through redistribution, to overcome a local activation threshold: $z(x, t) > z_c(x, t)$. For a large class of models, this implies that if $H(x, t)$ defines the time-integrated activity, $H = \int^t \rho(x, \tau) d\tau = \int^t \Theta(z(x, \tau) - z_c(x, \tau)) d\tau$, then after discretization H obeys the discrete *interface equation*

$$H(x, t+1) = \begin{cases} H(x, t) + 1, & f(x, t) > 0, \\ H(x, t), & f(x, t) \leq 0, \end{cases} \quad (1)$$

where f denotes the local 'force' acting on the interface [4]. This can be recast in the form

$$\frac{\Delta H}{\Delta t} = \Theta(\nu \nabla^2 H + \eta(x, H) + F(x, t) - F_c). \quad (2)$$

The Laplacian comes from the average redistribution of grains, and a constant ν takes into account the specific updating rules of the system. η is a *quenched noise term* that originates from the random rules of sandpiles.

$F(x, t)$ measures the external drive and changes on the slow-time scale, and F_c is the toppling threshold written as a force acting on the interface. By casting the dynamics of a sandpile in the form of a driven interface in a random environment (η) one sees that the SOC critical point is reached under the combined action of a slowly-increasing external force $F(x, t)$ and the boundary conditions, $H = 0$, which amount to the loss of grains. This is a slightly unusual case of a *depinning transition* of the quenched Edwards-Wilkinson universality class, since the macroscopic shape of the interface is parabolic (in 1D) [4]. The avalanche picture in an ordinary depinning transition [5–8] is however different since the translational invariance is here broken as manifested already in the average interface profile - which tells us that the activity density peaks in the bulk, in the center of the system.

The connection of SOC to non-equilibrium phase transitions can be made both in the interface context and in the realm of absorbing state phase transitions, exemplified by the contact process and various reaction-diffusion models [3,9]. One way to classify SOC models is to consider the noise correlator in the presentation at hand. Such analysis however assumes certain symmetries included in the representation (the QEW Langevin equation; the Langevin equation describing the active site density). A pertinent question thus arises: what happens if the ensemble, in which SOC is observed, is varied with respect to its fundamental symmetries? In this work we illustrate this by analyzing the outcome for the Kardar-Parisi-Zhang universality class. The difference between the QKPZ and the EW equations (or a non-linear Langevin equation compared to a linear diffusion equation) is that the diffusion equation is insensitive to most initial profiles due to the fundamental symmetries of the equation, while in the QKPZ case the growth component perpendicular to the interface slope is always non-zero. This means that there will be a new history dependence in the QKPZ interface which is absent from the EW dynamics and from usual absorbing state phase

transitions.

Consider, in analogy to the sandpile interface representation, the quenched KPZ equation [10] which reads

$$\frac{\Delta H}{\Delta t} = \Theta(\nu \nabla^2 H + \frac{\lambda}{2} (\nabla H)^2 + \eta(\mathbf{x}, H) + F(x, t)), \quad (3)$$

where the nonlinearity proportional to λ has been added to the QEW equation. Note the step function that enforces the constraint that the interface cannot propagate backwards. In the case of the sandpile equation, it also discretizes the interface velocity to zero or unity which in the absence of mixing by randomness creates an important Abelian symmetry and thus becomes crucial in that case [11]. The external drive is in the following taken to be uniform in space, $F(x, t) \rightarrow F(t)$ and the noise to be quenched and delta-correlated, $\langle \eta(\mathbf{x}, H) \eta(\mathbf{x}', H') \rangle = 2D \delta^d(\mathbf{x} - \mathbf{x}') \delta(H - H')$. Equation (3) has to be augmented with suitable boundary conditions in order to reach a steady-state. As in the QEW or sandpile ensemble, we use the selection $H(x, t) = 0$ at $x = 0, x = L + 1$ (in 1+1 dimensions) instead of e.g. periodic boundary conditions. In the case of such ordinary boundary conditions Eq. (3) has a depinning transition at a critical F_c . The exponents depend on whether λ approaches zero with $\Delta F \equiv F - F_c \rightarrow 0$ or not, and in the latter case we have a true QPKZ depinning transition [10,12].

An interface evolving from a flat boundary condition will develop a non-zero roughness and finally stops due to the influence of boundary conditions. The roughening, the development of average local slopes, depends on the sign of λ . To reach SOC-like conditions, the separation of timescales, or a vanishingly small but positive interface velocity (average activity level) $v = 0^+$ one has to choose the right way of driving the system, $F(t)$. For $F(t) > 0$ the interface becomes *unstable* if $\lambda > 0$ and $\frac{dv}{dt} > 0$. This breaking of up/down symmetry, absent in the continuum QEW model, shows the first sign that the possible SOC state in the QKPZ equation is different. If $\lambda < 0$ it becomes possible to take the SOC limit of vanishingly slow external drive,

$$F(t) = \zeta t, \quad \zeta \rightarrow 0 \quad (4)$$

from which follows that a separation of time-scales happens, similarly to the QEW or normal sandpile case. In the following we investigate the ensuing interface dynamics.

To this end, a cellular automaton [13] version of Eq. (3) is defined as follows. Let f_i be a microscopic force at the discretized sites $x \rightarrow i$, such that for $f_i > 0$ i topples. f_i reads in 1D

$$\begin{aligned} f_i(t) = & \nu [H_{i+1}(t) + H_{i-1}(t) - 2H_i(t)] \\ & + \frac{\lambda}{4} ([H_i(t) - H_{i-1}(t)]^2 + [H_{i+1}(t) - H_i(t)]^2) \\ & + F(t) + \eta_{i,H_i}. \end{aligned} \quad (5)$$

This can be interpreted, in analogy to SOC ones, as a *QKPZ sandpile* where a site gives 2ν particles or

units of energy to its neighbors once it topples, and the toppling criterion also compares the integrated activity at site i to its neighbors. In the interface picture $H_i(t+1) = H_i(t) + \Theta(f_i(t))$. With this definition, $H(x, t) = \int^t \rho(x, \tau) d\tau$ maps the discrete QKPZ equation to the 'sandpile' and vice versa. Notice that the nonlinearity, proportional to λ , above is discretized in a particular way, to avoid the numerical instabilities of the QKPZ equation in a reasonable fashion [14].

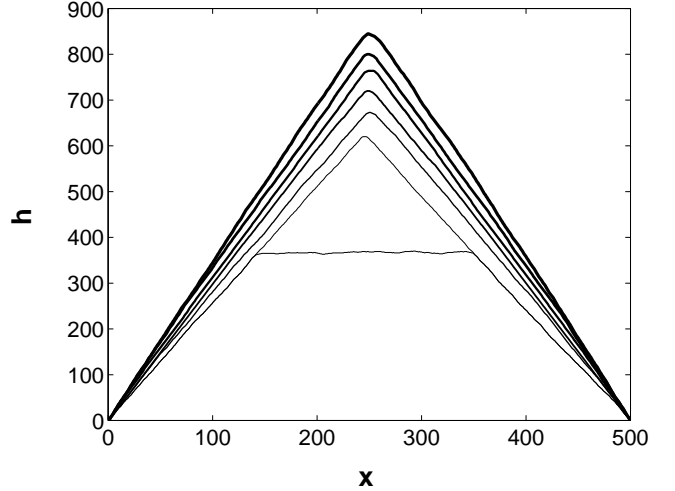


FIG. 1. Typical interface configurations for a 1D system of 500 sites. The one with the flat top shows an unstable one from the initial growth event before the first 'triangle' is created. The other configurations are stable, from every 20000th time step.

Fig. 1 shows a series of snapshots from a simulation of the QKPZ equation with $\eta_{i,H_i} = \pm g$ with equal probability. This describes random toppling thresholds that change after each toppling in the sandpile language. The system is driven in such a way that $F(t)$ is increased after an avalanche has relaxed (defined in the usual way by the stoppage of all activity), so that one site becomes active, and the interface advances. It is evident that the dynamics of such a system consists of at least of the development of an initial profile, and the subsequent phase(s). The macroscopic shape of the QKPZ interface is to first order triangular in 1+1-D as expected with $\lambda < 0$. The slope follows from the different terms in Eq. (3). For a flat slope the surface tension is negligible, and the slope arises from the balance of the nonlinearity and the driving force. This gives $\langle |\nabla h| \rangle = \sqrt{2\zeta t/\lambda}$. The development of such a profile, determined by the symmetries of the interface equation, is analogous to the development of the steady-state grain configuration in ordinary SOC sandpiles from an empty system. Next we discuss the phase that appears after the initial transient.

As in ordinary SOC, avalanches are characterized by the duration T , area l , and number of topplings s (the

number of times sites advance). The initial growth, giving rise to the triangular shape, is neglected. We obtain for the avalanche sizes in this regime the result shown in Fig. 2 for four system sizes. The size distribution has *asymptotic power law decay* with a measured exponent of $\tau_s = 2.5 \pm 0.1$ with $P(s) \sim s^{-\tau_s}$. Due to the large τ_s exponent the average avalanche size is not dependent on L , unlike in usual SOC sandpile models.

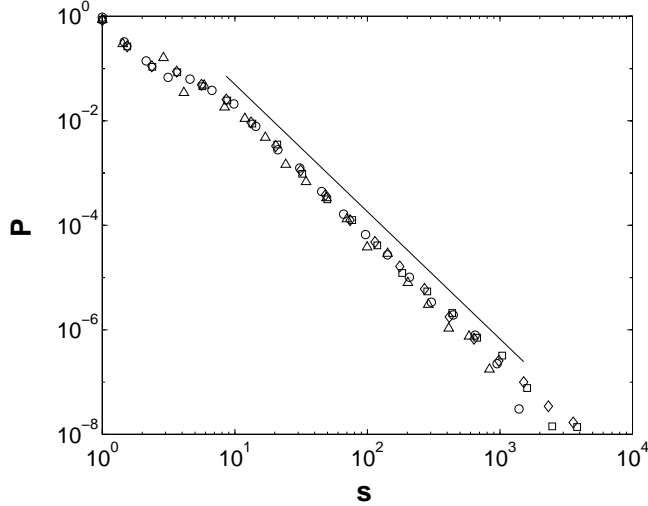


FIG. 2. Probability distribution function of the avalanche sizes for 1D ensembles. System sizes are 250, 500, 750, and 1000 for \triangle , \circ , \square , and \diamond , respectively. The parameters are $\nu = 20, \lambda = -4, g = 10$. Dynamics was only followed for configurations with average interface slopes less than 10 (see text). The parallel line indicates the region of power law fitting resulting in an exponent of -2.5 ± 0.1 .

However, the avalanches are time-translation invariant only *in the average sense*, due to the role of the average interface slope m . The avalanche sizes are plotted versus time on Fig. 3. On the same diagram, the standard deviation D of the local slope is also shown.

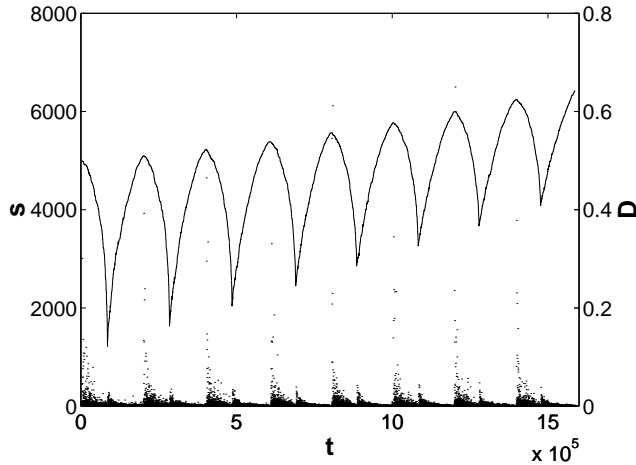


FIG. 3. Avalanche sizes s versus time and the standard deviation of the local slope D . $\nu = 20, \lambda = -4, g = 10$ and the system size is 1000. The correlation between the two quantities is obvious.

The largest avalanches take place when the roughness of the interface D is the largest. Smaller, but still relatively large avalanches develop where the sides of the triangular interface are smooth. The local slopes, i. e. $|H_i - H_{i-1}|$ alternate between n and $n + 1$, where n is a positive integer. It is not surprising that a smooth interface evokes large avalanches, because there are no fluctuations along the surface that would stop an upwards propagation of the avalanche. When D is the smallest, the first few avalanches start from either bottom of the triangle and propagate up to the top, increasing the interface height by one at every site. The really large avalanches occur at the maxima of D . They typically do not increase the average gradient of the side, but only the height of interface evenly along the side. In spite of the extra slope-dependence, there is no characteristic size as is typical of SOC and the correlation length equals the system size. The period of the avalanches is simply related to the squared system size. This is since the area covered by all the avalanches between two integer values of m is proportional to L^2 , and, the average avalanche size and duration are of the order of unity: $\langle s \rangle \sim \mathcal{O}(1)$ and $\langle T \rangle \sim \mathcal{O}(1)$.

The support or the area of the avalanche is as usual defined by the number of sites that have toppled at least once during an avalanche. Notice that an avalanche always tends to spread upwards, and thus in 1D the starting and final, extremal sites usually give the area directly. Sometimes, the Laplacian makes it so that an avalanche can propagate over the top of the 'triangle'. We find that the probability of starting an avalanche linearly increases with the location of a site and the probability of an avalanche to stop grows linearly also as the top is approached.

The area of the avalanches, defined as $l = i_r - i_l + 1$, is expected to follow a similar power law as the avalanche sizes do and one obtains that $\tau_l \sim 3.0 \pm 0.1$. The avalanche lifetime T is the time that elapses between two successive stationary states in the system and also behaves as a power-law, $P(T) \sim T^{-2.9 \pm 0.2}$. Due to the fact that the average avalanche properties are defined by the small avalanches no analogy of the usual scaling relations between the exponents seems to exist.

The above results have, however, been obtained in just a window of time. Consider an interface (side of the triangle) with an uniform slope m and an avalanche which has just started to propagate and reached site i . The local force at site i , at time t , becomes $f_i(t) = \nu(m - 1 - m) + \frac{\lambda}{4}[(m - 1)^2 + m^2] + F + \eta_i$ and at $i + 1$ $f_{i+1}(t) = \nu[m - (m - 1)] + \frac{\lambda}{4}[m^2 + (m - 1)^2] + F + \eta_{i+1} = \nu + \frac{|\lambda|}{4}(2m - 1) - \frac{|\lambda|}{4}2m^2 + F + \eta_{i+1}$. Assuming that on

average on an even interface F balances the local forces for slope m ($F \approx \frac{|\lambda|}{4} 2m^2$) and neglecting the noise fluctuations, we find a critical slope

$$m_{cr} \approx \frac{2\nu}{|\lambda|} + \frac{1}{2}. \quad (6)$$

This means that the cell at i may stay active for the next updating step at time $t + 1$ when $m > m_{cr}$. The natural progress of avalanches is now such that the site at $i + 1$ is normally always activated if the interface is smooth enough. In this phase the site at $i + 1$ gets active and topples at $t + 1$, but at the same time $H_i \rightarrow H_i + 1$ as well. Thus, a short region of the interface with a smaller gradient will be formed and starts to propagate upwards, giving rise to very large avalanches. Since these are more difficult to induce, the majority of the avalanches are of size unity, and tend to smoothen out the interface fluctuations. The avalanche statistics data presented previously is restricted to systems with a maximum slope of 10: the critical slope for those systems is $m_{cr} \approx 2 \cdot 20/4 + 1/2 = 10.5$. In this regime above the critical slope m_{cr} , the scaling structure of avalanche behavior is lost, and the growth process produces either extremely large or very small avalanches. This feature makes it prohibitively difficult to take this regime under closer scrutiny with numerical simulations. The time to reach m_{cr} can be estimated in two ways depending on whether one uses macroscopic time or 'SOC' time (counting the number of avalanches). With a uniformly, but very slowly increasing force F the critical slope is reached at the same time regardless of the system size L . In contrast, since the average size of an avalanche is independent of L (recall that $\tau_s > 2$), it follows that the number of avalanches n_{cr} to reach m_{cr} will depend on L as $n_{cr} \sim L^2$.

The previous results illustrate the nature of SOC in the QKPZ universality class. The combination of slow drive and boundary pinning chooses a certain symmetry for the average interface profile. This can be further elaborated by considering the continuum equation, and writing the interface field on one of the sides of the triangle as $H(x, t) = m(t)x + \delta H(x, t)$. Inserting this into the QKPZ equation we obtain for δH

$$\frac{\partial \delta H(\mathbf{x}, t)}{\partial t} = \nu \nabla^2 \delta H + \lambda m(t) \nabla \delta H + \frac{\lambda}{2} (\nabla \delta H)^2 + \eta(\mathbf{x}, H), \quad (7)$$

where the mean-field solution for H has been subtracted from the equation and the result is valid for intermediate times $\delta t \ll t$. We discover that the externally imposed slope (by the combination of F and $H = 0$ at the boundaries) *changes the effective interface equation* by creating a term linear in $\nabla \delta H$, that will dominate over the KPZ-nonlinearity. The situation is thus exactly analogous to depinning transitions in the presence of an anisotropy, discussed by Kardar, Dhar, and Tang [15]. This explains qualitatively why the avalanche behavior at criticality,

at the SOC depinning transition, is different from that of the bulk depinning transition for the original equation. Regardless of whether the SOC ensemble differs from the translationally invariant one for ordinary SOC sandpiles, it is thus clear that in the case of SOC obtained with a similar recipe in QKPZ-systems the two ensembles do not share the same exponents. Should it be possible to write an activity-based description for the QKPZ universality class, this implies that the field theory should have a different structure in the two cases, in contrast to the connection between the QEW and absorbing state phase transitions with a conserved field [16].

Above, we have concentrated on a cellular automaton for the QKPZ equation since as discussed it is related to a microscopic 'activity' picture, or a "QKPZ sandpile". The slow-drive SOC-depinning limit can be taken also in the continuum version. Our investigations indicate that the same phenomenology of symmetry breaking persists in that case as well, though the actual exponents in the second phase before the critical slope is reached differ as Δh can now have arbitrary values and the avalanche properties change. The analysis of the continuum model is hampered by well-known numerical instabilities that develop once the smoothing effect of the Laplacian is reduced - which is inevitable here due to the increasing average slopes. We have also studied the two-dimensional case. While there, with periodic boundary conditions in one direction, and SOC ones in the other, are interesting details concerning the geometry of avalanche spreading, the basic physics is the same as in 1D.

In conclusion, in this paper we have analyzed the behavior of interfaces in the QKPZ universality class in the presence of conditions that produce self-organized criticality. Spatial and temporal invariance are broken by the slow drive and the dissipative pinning boundary conditions, giving rise to a macroscopic interface shape. The shape, in combination with the nonlinearity, results in the creation of a term linear in δh in the effective equation that governs the physics of avalanches. In contrast to usual SOC sandpiles we find that there are two avalanche regimes depending on the microscopic dynamics, where the second one fails to show critical scaling seen in the first. The ensemble in which the criticality appears is fundamentally different from the usual depinning one and is related to the anisotropic QKPZ class [15].

Partial support of OTKA T029985 is acknowledged.

-
- [1] P. Bak, C. Tang and K. Wiesenfeld, Phys. Rev. Lett. **59**, 381 (1987); Phys. Rev. A **38**, 364 (1988); P. Bak, *How Nature Works* (Copernicus, New York, 1996).
 - [2] T. Hwa and M. Kardar, Phys. Rev. Lett. **62**, 1813 (1989); G. Grinstein, D.-H. Lee and S. Sachdev, Phys. Rev. Lett. **64**, 1927 (1990); L. Gil and D. Sornette, Phys. Rev. Lett.

- 76**, 2738 (1996); A. Montakhab and J.M. Carlson, Phys. Rev. E **58**, 5608 (1998).
- [3] M.A. Muñoz, *et al.*, cond-mat/0003285; R. Dickman, *et al.*, Braz. J. Phys. **30**, 27 (2000).
- [4] M.J. Alava and K.B. Lauritsen, cond-mat/9903349; Europhys. Lett. **45**, 453 (2001).
- [5] T. Nattermann, *et al.*, J. Phys. (France) II **2**, 1483 (1992); H. Leschhorn, *et al.*, Ann. Physik **7**, 1 (1997).
- [6] H. Leschhorn, Physica A **195**, 324 (1993).
- [7] O. Narayan and D.S. Fisher, Phys. Rev. B **48**, 7030 (1993).
- [8] P. Chauve, T. Giamarchi and P. Le Doussal, Phys. Rev. B **62**, 6241 (2000).
- [9] M. Rossi, R. Pastor-Satorras and A. Vespignani, Phys. Rev. Lett. **85**, 1803 (2000); R. Pastor-Satorras and A. Vespignani, Phys. Rev. E **62**, R5875 (2000).
- [10] A.L. Barabasi and H.E. Stanley, *Fractal Concepts in Surface Growth* (Cambridge Univ. Press, Cambridge, 1995) and references therein.
- [11] D. Dhar, Physica A **263**, 4 (1999) and references therein.
- [12] N. Neshkov, Phys. Rev. E **61**, 6023 (2000).
- [13] H. Leschhorn, Phys. Rev. E **54**, 1313 (1996).
- [14] T.J. Newman and A.J. Bray, J. Phys. A **29**, 7917 (1996).
- [15] L.-H. Tang, M. Kardar, and D. Dhar, Phys. Rev. Lett. **74**, 920 (1995).
- [16] M.J. Alava and M.A. Muñoz, cond-mat/0105591.